CHARGED CLUSTER MODEL AS A NEW PARADIGM OF CRYSTAL GROWTH

Nong-M. Hwang[a,b] In-D. Jeon[a] and Doh-Y. Kim[a]

[a]Center for Microstructure Science of Materials, School Mater. Sci. & Eng.

Seoul National University, Seoul 151-742, Korea

[b]Korea Research Institute of Standards and Science

P.O. Box 102, Yusong, Taejon 305-600, Korea

A new paradigm of crystal growth was suggested in a charged cluster model, where charged clusters of nanometer size are suspended in the gas phase in most thin film processes and are a major flux for thin film growth. The existence of these hypothetical clusters was experimentally confirmed in the diamond and silicon CVD processes as well as in gold and tungsten evaporation. These results imply new insights as to the low pressure diamond synthesis without hydrogen, epitaxial growth, selective deposition and fabrication of quantum dots, nanometer-sized powders and nanowires or nanotubes. Based on this concept, we produced such quantum dot structures of carbon, silicon, gold and tungsten. Charged clusters land preferably on conducting substrates over on insulating substrates, resulting in selective deposition. If the behavior of selective deposition is properly controlled, charged clusters can make highly anisotropic growth, leading to nanowires or nanotubes.

Key words : charged cluster, crystal growth, thin film, quantum dot, nanowire, nanotube

1. Introduction

It is generally believed that the growth unit of a crystal or a thin film is either an atom or a molecule. The atom first adsorbs on the terrace, diffuses to the ledge and finally becomes the crystal at the kink [1, 2]. Drastically a different way of crystal growth was suggested by Glasner et al. [3-6] during their study on the crystal growth of KBr and KCl in the presence of Pb^{2+} in an aqueous solution. In this case, the nanometer-size nuclei are formed in the solution and they become the growth unit. They confirmed the formation of these invisible clusters in the solution by a thermal method, where the heat generated during cluster precipitation from the solution is measured. They showed that an almost perfect crystal grew by orderly packing or self assembly of these nuclei with perfection of a crystal increasing with decreasing size of nuclei. Their suggestion was so revolutionary that it received severe criticism [7] and has been neglected in the crystal growth community.

Sunagawa [8] made a similar suggestion that the growth unit of synthetic diamond is not an atom but a much larger unit. According to the analysis of periodic bond chain (PBC), the (111), (110) and (100) plane surfaces of diamond are flat (F), stepped (S) and kinked (K) faces, respectively. The growth morphology of diamond by atomic deposition should be the octahedron surrounded by the slowest growing (111) planes. All natural diamonds satisfy this morphology predicted by PBC analysis. The synthetic diamonds produced either by a high pressure process or by a low pressure process are characterized by frequent evolution of the (110) or (100) planes, resulting in truncated octahedron or cubic shapes. Besides, the macrosteps of synthetic diamonds are wavy instead of being straight. Based on these observations, Sunagawa suggested that

although the growth unit of natural diamonds is an atom, the growth unit of synthetic diamonds is much larger than individual atoms. He further presumed that the size of the growth unit would be comparable to the height of the wavy macrosteps. This ingenuous suggestion also has not been taken seriously in the diamond community because its idea is too revolutionary.

Based on thermodynamic, kinetic and morphological analyses of the diamond CVD, Hwang et al. [9-13] suggested a charged cluster model (CCM), which is a very similar concept to the growth mechanism suggested by Glasner et al. [3-6] and Sunagawa [8]. In the CCM of the CVD diamond, charged diamond clusters containing hundreds to thousands of atoms are suspended like colloidal particles in the gas phase and become a building unit of diamond crystals. The stability of diamond can be increased over that of graphite by the high capillary pressure inside the cluster and further by charge, which makes a strong ion-induced dipole interaction for the dielectric diamond cluster [14, 15].

Recently, the existence of these hypothetical negatively charged nanometer clusters containing hundreds of carbon atoms [16, 17] was experimentally confirmed. It was shown that the size of clusters increased with methane concentration. Small clusters produced diamond crystals with well-developed facets while large clusters produced ball-like or cauliflower-shaped diamonds, as had been predicted in the CCM [11, 13].

The CCM was successfully applied to the silicon CVD [18-20], zirconia CVD [21], thermal evaporation coating of tungsten [22] and gold [23]. According to the morphological analysis of films on the substrate materials with a high charge transfer

rate (CTR), the CCM is also valid in the laser ablation and the sputtering processes [24] The validity of the CCM appears to be general in the thin film process.

In this paper, the implications of the CCM regarding crystal growth will be described with particular emphasis on epitaxial growth, nano-structured materials, selective deposition, nanowire or nanotube growth and quantum dot fabrication.

2. Experimental confirmation of charged clusters in the deposition reactor

The CCM states that the charged clusters of nanometer size are usually formed in the gas phase in a typical processing condition of thin films. Such clusters are difficult to detect because of their nanometer size, which is too small for appreciable intensity of light scattering and too large for the quadruple mass spectroscopy. This is why the existence of these clusters has been unnoticed so far. A special apparatus should be used to detect them. A time-of-flight (TOF) mass spectroscopy designed for the high mass would be ideal. Since the accuracy of mass resolution need not be so high as TOF and the simple apparatus such as a Wien filter or an ion-mobility analyzer is suitable.

The pressure of CVD or other deposition reactors is typically in the range of 10^{-1} ~ 10^{2} Torr while the pressure in the mass analysis chamber should be less than 10^{-5} Torr. Therefore, the gas or the clusters should be extracted through an orifice (~ 1 mm in diameter) by differential pumping from the deposition reactor to the mass analysis chamber. Using a Wien filter and an ion-mobility analyzer, recently we experimentally confirmed the existence of the hypothetical charged carbon clusters suspended in the hot filament diamond CVD reactor [16, 17] as shown in Fig. 1 and Fig. 2.

Fig. 1 shows the mass distribution of the negatively charged carbon clusters suspended in the hot filament diamond CVD reactor under 6 Torr at the filament

temperature of 2100°C with a gas mixture of 1.5%CH_4-98.5%H_2. The mass distribution was measured by a Wien filter in combination with an ion-mobility analyzer [16]. In order t maintain the pressure of the measuring chamber below ~ 10^{-5} Torr, two-stage differential pumping had to be used. Most clusters were negatively charged with the amount of positively charged clusters being negligible in the hot filament reactor. The peak of Fig. 1 corresponds to ~ 3000 atomic mass unit (amu), which is equivalent ~ 250 atoms. The number density of charged clusters in the reactor was estimated to be ~ 10^6 mm^{-3}.

Figure 2 shows the mass distribution of charged carbon clusters with four different methane concentrations of 1%, 1.5%, 3% and 5% CH_4 [17]. In this case, the mass distribution was converted from the energy distribution of charged clusters based on the pre-determined relation between the mass of clusters and their velocity following the scheme of Gerhardt and Homann [25]. Clusters of ~ 3000 amu are dominant for low methane concentrations (1% and 1.5 CH_4) while the mass distribution for the higher methane concentrations (3% and 5% CH_4) was much broader with an appreciable number of large clusters (~ 18000 amu). ~ 3000 and ~ 18000 amu correspond to ~ 250 and ~ 1500 carbon atoms, respectively.

During the measurement of the energy distribution, diamonds were deposited *in situ* on the Mo substrate placed on the orifice near the hole with a substrate temperature of 750°C. Figures 3(a) and 3(b) show the scanning electron microscopy (SEM) images after deposition for 1 hr at 1% and 3% CH_4, respectively. The results indicate that clusters of ~ 3000 and ~ 18000 amu deposit diamonds with well-defined facets and a ball-like or cauliflower-like shape, respectively. Development of crystal facets results from the anisotropic growth rate with crystallographic directions, implying that small

clusters undergo layer-by-layer growth. In this case, clusters will undergo epitaxial coalescence on the growing surface. Development of cauliflower-shaped diamonds results from the isotropic growth rate, implying that large clusters tend to undergo adhesive-type growth. Large clusters will frequently fail epitaxial coalescence and tend to make grain boundaries with the growing surface, leading to nanostructure.

In relation to dependence of the growth mode on cluster size, works of Yoshida et al. [26-29] is worth mentioning. They studied the surface morphology of epitaxial $YBa_2Cu_3O_{7-x}$ films prepared by thermal plasma flash evaporation by scanning tunneling microscopy (STM). The main deposition species were the clusters ranging from 0.3 to 9 nm. They observed that small clusters (1 ~ 2 nm) undergo epitaxial spiral growth, medium size clusters (3 nm) become epitaxial 2-dimensional nuclei and large clusters (larger than 3 nm) become non-epitaxial island grains. These results imply that spiral steps of monoatomic height observed by STM are not necessarily an indication of atomic unit growth but can be formed by cluster unit growth. Besides, the results show that the layer-by-layer growth mode can also be achieved by cluster unit deposition.

The mass analyzer such as TOF or Wien filter needs a high vacuum ($< 10^{-5}$ Torr). However, differential mobility analyzer (DMA) operates at atmospheric pressure and can measure the size range of 1 ~ 20 nm if specially designed for nanosize measurement. Using a nano-DMA, the size distribution of charged diamond clusters of a few nanometers was measured during the oxyacetylene flame synthesis of diamond [30]. The results of nano-DMA agreed with the cluster size measured by transmission electron microscopy (TEM) after capturing clusters on a TEM grid [30].

Using a DMA and a particle number counter, Adachi et al. [31-35] and Okuyama et

al. [36-40] made extensive studies on the size distribution of clusters suspended in the gas phase in the CVD reactor. During the SiO_2 CVD using tetraethylorthosilicate (TEOS) as a precursor, Adachi et al. [31-35] found out that the film did not grow under conditions that the clusters were not detected in the gas phase. Further, they observed that the growth rate of films increased with increasing number density of clusters in the gas phase. Okuyama et al. [40] observed that under the film processing conditions generating the small cluster of a few nanometers, the film surface was smooth while under the conditions generating the coarse ones larger than 10 nanometers, the film surface was irregular.

3. Gas phase nucleation in the thin film reactor

The formation of charged clusters in the thin film reactor indicates that gas phase nucleation takes place under typical conditions of film deposition. Normally, it is thought that the gas phase nucleation is homogeneous nucleation, which is far from being true. In fact, the homogeneous nucleation in the gas phase is very difficult to achieve as had been well revealed in the Wilson cloud chamber experiment [41-44].

When the Wilson cloud chamber [41] was first invented, the purpose was to test the Volmer's theory of homogeneous nucleation. The Wilson chamber is a simple adiabatic expansion system, which induces supersaturation of the water or alcohol vapor. In the first expansion, nucleation was not homogeneous but heterogeneous on dust. After several expansions, the dust-free clean vapor could be prepared but still nucleation was not homogeneous but heterogeneous on ions. Even after repeated expansions, ion-induced nucleation could not be avoided. Later it was found out that ions are

continuously generated by natural radio activity and cosmic rays and a steady state concentration of ~ 10^3 ion pairs cm^{-3} is maintained in air. Nucleation on ions was so sensitive that this fact was utilized in locating the track of the high energy particles, contributing to the discovery of many particles such as positron.

Considering that the ion-induced nucleation could not be avoided even in dust-free clean air at room temperature, it is highly probable that the gas phase nucleation might be induced by ions in thin film reactors. According to our current measurements by the Faraday cup in the thermal CVD and evaporation reactors, at least ~ 10^6 ion pairs cm^{-3} are typically measured under thin film deposition conditions [23]. Ion concentrations in the hot filament and plasma diamond CVD reactors are, respectively, three and six orders of magnitude higher than those in thermal CVD and evaporation reactors.

It should be noted that nucleation in the gas phase is induced not only by ions but also by other sources such as photo-excited species. Photo-induced nucleation is known to be much more powerful than ion-induced nucleation in triggering nucleation in the gas phase [45, 46]. In the case of nucleation of pure water from its supercooled vapor, photo-induced nucleation was detected at supersaturations as low as 1.00042 [46].

When the ion-induced nucleation takes place in the cloud or the bubble chambers for locating the track of the high enregy particles, the nuclei instantly grow into a visible size. In this case, the amount of flux for nuclei to grow is enormously large compared to the concentration of ions. When the amount of flux to precipitate is small compared to the concentration of ions as in the case of a thin film process, the charged nuclei do not grow much but might maintain their nanometer size during their residence time in the gas phase. The resultant films deposited by these clusters are not distinguishable from those deposited by individual atoms or molecules.

Then why do we choose the processing condition where the nanometer clusters are formed in the gas phase during the thin film process? Or why is the formation of charged clusters so general in the thin film process? The reason is in the growth rate of thin films. In order to suppress ion-induced nucleation in the gas phase, the supersaturatioin should be maintained to be low, which results in a negligible deposition rate. How slow would be the growth rate for supersaturation low enough to suppress the gas phase nucleation? The results by Adachi et al. [31-35] provide a clear answer for this question. They observed that the film did not grow under the conditions where the gas phase nucleation was suppressed.

Another good example, where the film growth rate without gas phase nucleation can be estimated, is the old method of metastable diamond growth [47, 48] before the discovery of the gas activation process. In this method, the metastable diamond grew on the diamond seed with thermal decomposition of the gas mixture of methane and hydrogen. The underlying principle is that the growth barrier of diamond would be lower than the nucleation barrier of graphite on the diamond seed. Considering the capillary effect in the nucleation stage, the growth barrier of diamond is expected to be much lower than the nucleation barrier of graphite on the diamond surface and the graphite nucleation on the diamond surface is not expected. But if the gas phase nucleation takes place, graphite might nucleate dominantly over diamond in the process not using gas activation. Once the graphite phase formed in the gas phase and landed on the diamond surface, the graphite covered an entire diamond surface because of its much higher growth rate than that of diamond. For further growth of diamond, the graphite phase had to be etched away by hydrogen. Therefore, the process was cyclic: etching and growth. It should be noted that the supersaturation had to be kept low to

minimize the gas phase nucleation. Under this condition, the growth rate of diamond films was a few angstroms per hour. This growth rate is roughly four orders of magnitude slower than the growth rate of diamond using the gas activation in the presence of charged clusters in the gas phase.

4. Generation of charge during thin film depositions

Although the ion generation mechanism in hot filament and plasma CVD reactors is clearly understood, the mechanism is not yet clear in thin film reactors of thermal CVD and evaporation at relatively low temperature. According to our electric current measurements by a Faraday cup, the ion concentration increases abruptly with cluster formation. In the deposition process by thermal evaporation, the ion current increases abruptly just above the melting point of the material to evaporate. In the CVD process, the ion current increases abruptly when the precursors start to decompose. Magnusson et al. [49] also observed an anomalous charging behavior of gold nanoparticles above 600°C.

One possible explanation of our experimental observation is as follows. Clusters have a low ionization potential and a high electron affinity, both of which approach a work function value of the bulk. In the supersaturated state for film deposition, embryonic clusters will be generated. They will be easily ionized when in contact with the hot surface by surface ionization, which is described by Saha-Langmuir equation [50]. The surface ionization is also possible in the interactions between clusters and gaseous atoms, molecules or compounds. Once the embryonic clusters become charged, they can grow above the critical nucleus size by ion-induced nucleation in the presence of appreciable supersaturation for deposition. According to this explanation, ion

generation and clustering affect each other; the electric charge triggered by embryonic clusters also triggers the embryonic clusters to grow into stable nuclei.

5. Effect of charge in charged clusters

In order to describe the effect of charge in the CCM, behaviors between neutral and charged clusters should be compared. When the clusters are formed by supersonic expansion, electric charging of clusters is not expected and dominantly neutral clusters would be generated. Neutral clusters undergo Brownian coagulation and grow into a fractal structure by diffusion-limited-aggregation (DLA) [51]. They would grow instantly into macro-particles during their residence time in the reactor. Charged clusters of the same sign, however, do not coagulate and suspend like colloids in the gas phase during their residence time in the reactor, maintaining their nanometer size. Besides, these charged clusters undergo deflocculation settling, resulting in 3-dimensional self-assembly into a compact structure.

Recently, self-assembly of nanoparticles has been hot issues [52-56]. Self-assembly can be either 2-dimensional (2-D) or 3-dimensional (3-D), which has been clearly demonstrated in zeolite nanoparticles [56-58] and submicron latex particles [59-61]. In some cases, the assembly is so perfect that the resulting film becomes transparent [57, 59] or has a superlattice, which is investigated by small–angle X-ray scattering [61]. Also Cu, Ag and Au monodisperse nanoparticles suspended in solution were shown to undergo self-assembly into a perfect superlattice such as face-centered cubic (FCC) [54, 57, 59, 62-64].

In this colloidal processing, the self-assembly is done mostly at room temperature

and the individual nanoparticles have their own orientations in the superlattice and keep their identity. If the self-assembly is done at a relatively high temperature as in the thin film process, however, individual nanoparticles undergo epitaxial coalescence on the growing surface and lose their identity. If the growth by 3-D self-assembly is achieved by repeated 2-D self-assembly, crystals with well-defined facets will be grown. The resulting films cannot be distinguished from those grown by atomic unit.

The effect of charge on the film formation is well represented in the deposition behavior between substrates with a high and a low charge transfer rate (CTR). On the substrates with a high CTR such as Pd, Ir, Rh, Pt, Fe and Ni, the porous skeletal soot structure is evolved while on the substrates with a low CTR such as Si and insulating materials, the dense film is evolved [11, 65, 66]. On the substrates with a high CTR, the charge is lost just before landing and the resultant neutral clusters deposit on the substrate like flocculation, resulting in a porous structure. On the substrate with a low CTR, however, the charge is retained in the clusters during landing and clusters undergo highly compact and regular packing of 3-D self-assembly, resulting in dense films.

Fig. 4 shows these aspects in the silicon CVD [24]. After 3 minutes of silicon CVD with a Ni substrate, the porous silicon deposited (Fig. 4(a)) while after 30 minutes, the large crystalline silicon grew on the porous silicon (Fig. 4(b)). In the initial stage, the porous silicon deposited because of a high CTR of the Ni substrate. But after the Ni substrate is covered with the porous silicon with a low CTR, the Si surface would have the low CTR. Therefore, dense silicon particles can grow on the initially-deposited porous silicon.

Fig. 5 shows the effect of the CTR of substrates in the diamond CVD; the porous skeletal graphitic soot on Fe (Fig. 5(a)) and the dense diamond film on Si (Fig. 5(b))

[11]. In this case, the porous soot has a graphite structure and the dense film has a diamond structure. This result indicates that if charged diamond clusters lose charge to the substrate with a high CTR, they transform instantly into graphite clusters. The loss of diamond stability after losing charge was attributed to the loss of an electrical double layer at the surface of diamond clusters [11]. The electrical double layer can be formed on a dielectric diamond cluster while it cannot form on a conducting graphite cluster.

It should be noted that the high capillary pressure built up inside the nanometer carbon cluster increases the stability of diamond significantly so that the stability between diamond and graphite is very close [9, 67]. The slight increase in diamond stability by an electric double layer induced by charge can reverse the stability between diamond and graphite clusters [12, 14, 15]. In this respect, the presence of electric charge is essential to a low pressure synthesis of diamond. This concept is drastically different from the conventional belief that the production of atomic hydrogen is essential to a low pressure synthesis of diamond [68-70]. Recently, the low pressure synthesis of diamond was shown to be possible without hydrogen [71-73]. This fact supports the CCM, in which the electric charge rather than hydrogen is essential to low pressure synthesis of diamond [74].

It is known that nanometer sized diamonds exist in abundance in interstellar space [75, 76]. Their existence was confirmed in the meteorites. Other materials coexisting in the meteorites do not have their high pressure form and therefore, interstellar diamonds are thought to have nucleated under low pressure [76, 77]. The interstellar diamond dust is another example of low pressure formation of diamond in the absence or scarcity of

hydrogen. Considering that the interstellar space is a highly ionizing environment, the formation of interstellar diamonds might also be explained by the CCM [74].

Another effect of charge is on the size distribution of clusters. Charged clusters tend to have monodisperse clusters or nanoparticles, which are favorable for the self-assembly. The charge affects the size distribution in two ways. One is the inhibition of Brownian coagulation as in the case of colloid particles. The other is the modification of the Thompson-Freundlich equation by introducing the electrostatic interaction term. The free energy of the neutral clusters and its Thompson-Freundlich equation are expressed, respectively, as

$$\Delta G = -\frac{4\pi}{3} r^3 \Delta\mu + 4\pi r^2 \sigma \quad \text{and} \tag{1}$$

$$\ln\left(\frac{P}{P_\infty}\right) = \frac{V_m}{RT}\frac{2\sigma}{r}, \tag{2}$$

where P and P_∞ are the vapor pressure for the cluster of radii, r and ∞, respectively. V_m is the molar volume, σ is the surface energy and RT has its usual meaning. The free energy of the singly charged conducting cluster and its Thompson-Freundlich equation are expressed, respectively, as

$$\Delta G = -\frac{4\pi}{3} r^3 \Delta\mu + 4\pi r^2 \sigma + \frac{e^2}{2r} \quad \text{and} \tag{3}$$

$$\ln\left(\frac{P}{P_\infty}\right) = \frac{V_m}{RT}\left(\frac{2\sigma}{r} - \frac{e^2}{8\pi r^4}\right), \tag{4}$$

where e is the electric charge. Equation (4) indicates that the charged cluster cannot dissolve energetically.

In some case, the distribution of charged clusters become bimodal [23]. The evolution of bimodal evolution is attributed to the attractive Coulomb interaction

between two charged conducting clusters with a large size difference. The Coulomb interaction between two charged conducting clusters of the same sign is expressed as [78]

$$F = \frac{q_1 q_2 e^2}{4\pi\varepsilon_o d^2} - \frac{q_1^2 e^2 r_2 d}{4\pi\varepsilon_o \left(d^2 - r_1^2\right)^2} - \frac{q_2^2 e^2 r_1 d}{4\pi\varepsilon_o \left(d^2 - r_2^2\right)^2} + \cdots, \quad (5)$$

where the sphere of radius r_1 has a net charge q_1 and the other of radius r_2 has charge q_2; d is the distance between the centers and $1/4\pi\varepsilon_o$ the permittivity. Equation (5) indicates that two clusters with a large size difference can be attractive each other even though they carry the same sign. Therefore, large clusters continue to grow by coagulation with small clusters while growth of small clusters is suppressed, leading to bimodal size distribution.

6. Selective deposition behaviors of charged clusters

In the thin film process, it is frequently observed that the deposition is more favorable on conducting substrates than on insulating ones. Using this fact, the technique of selective deposition has been extensively used in microelectronics [79-83]. In spite of the technological importance of this phenomenon, its underlying principle has not yet been clearly understood.

According to the CCM, charged clusters are the major deposition flux. Because of charge, their landing behavior between conducting and insulating substrates is expected to be quite different. They will land on conductors easily but have difficulty in landing on insulators, especially when the gas phase is insulating. Kumomi et al. [79, 84, 85] observed that in the selective nucleation based epitaxy of silicon using the Si-Cl-H system, silicon deposited selectively on the SiN_x surface patterned on SiO_2. SiN_x is more

conducting or less insulating than SiO_2. This is why silicon did not deposit on SiO_2. They further observed that most silicon particles, which had deposited on SiN_x initially, etched away later. Only one silicon particle grew larger while all other silicon particles completely etched away. This phenomenon indicates that two irreversible processes of deposition and etching in opposite directions occur simultaneously.

This experimental observation is in contradiction with the second law of thermodynamics if the deposition unit is an atom. This puzzling phenomenon could be approached by the CCM [18]. Charged silicon clusters were suspended in the gas phase and deposited as silicon particles. Since the Si-Cl-H system has the retrograde solubility of silicon in the gas phase around the substrate temperature, the gas phase nucleation changes the driving force at the substrate temperature from being for deposition to being for etching. Therefore, between the gas phase and the substrate were exchanged two irreversible fluxes of silicon: atomic etching and cluster deposition.

In an initial stage, charged silicon clusters will deposit on the SiN_x surface which is electrically floated by SiO_2 and the electric charge will build up and be saturated in a later stage. When the SiN_x surface is saturated with charge, further deposition of charged silicon clusters is inhibited by Coulomb repulsion. Then, atomic etching will dominate and most silicon particles will etch away in a later stage. Exceptional growth of one large silicon particle was attributed to the Coulomb attraction between the large silicon particle and the charged clusters, which is given by Eq. (5).

The existence of silicon clusters in the gas phase was experimentally confirmed in the silicon CVD using the Si-Cl-H system [19]. Although silicon continued to deposit on the conducting surface, it deposited on the insulating surface in an initial stage and then etched away in a later stage [20]. These deposition behaviors can only be explained

by the CCM and indicates that the selective deposition is attributed to charged clusters.

7. Growth of nanowires by charged clusters

The selective deposition of charged clusters can make one-dimensional growth when charged clusters are more attractive to the tip than to the side wall of the deposits. This type of deposition can produce nanowires, nanowhiskers or nanotubes. One-dimensional growth is expected under the condition that the tip is more conducting than the side wall. The tip is made conducting when the metal particle is residing on it. Whisker growth of silicon using gold particles satisfies this condition [86, 87]. Recently, silicon nanowires were fabricated by laser ablation [88-91]. Zhang et al. [90] suggested a cluster-solid mechanism for growth of silicon nanowires based on their observation that Si nanoclusters had deposited on the cool finger during the growth of Si nanowires by laser ablation [90, 92].

However, if these clusters are neutral, they will undergo rapid Brownian coagulation in the gas phase and produce fractal or skeletal structures. In order to explain the highly anisotropic one-dimensional growth of nanowires, the additional effect of charge should be considered. Zhang et al. [90, 92] observed that a thin SiO_2 layer had formed on the outer surface of Si nanowires. The insulating SiO_2 layer is expected to inhibit the attachment of charged Si clusters on the side wall and appears to induce the preferential attachment of clusters on the tip.

We could also make Si nanowires in the CVD process using the gas mixture of SiH_4, HCl and H_2 [93]. The process was done under conditions of a substrate temperature of 950°C under a pressure of 10 Torr with a gas mixture ratio of $SiH_4 : HCl : H_2 = 3 : 1 : 6$.

On the conducting substrate, nanowires did not grow but typical Si films deposited as shown in Fig. 6(a). On the Si substrate, however, Si nanowires start to grow after 3 min as shown in Fig. 6(b). After 6 min of deposition, nanowires grew extensively on both Si and SiO_2 substrates as shown in Figs. 7(a) and 7(b), respectively.

8. Fabrication of quantum dots by charged clusters

According to the CCM, charged nanometer clusters or particles are formed in the usual thin film process without intentional efforts to generate them. Besides, as mentioned in the earlier section, charged clusters tend to be relatively uniform in size. Considering that spontaneously generated clusters in the thin film reactor are charged, the size can be selected by applying an electric field using differential mobility analyzer (DMA). Therefore, the nanometer clusters or nanoparticles of relatively uniform size can be easily fabricated based on the CCM. Si nanoparticles of relatively uniform size could be prepared by Si CVD [19]. Diamond nanoparticles were also prepared under the conditions of oxyacetylene flame deposition of diamond films [30]. W and Au nanoparticles were prepared by thermal evaporation [22, 23].

The cluster size largely depends on the reactor pressure, the residence time in the reactor, the amount of precipitation, and the amount of charge generated. For the given charge density, unipolar charge is much more effective than bipolar charge, in which case positive and negative clusters coagulate easily. We found out that carbon clusters formed in the hot filament (~ 2000°C) reactor are mostly negatively charged [16, 17]. The generation of unipolar charge is the advantage of the hot filament reactor in maintaining the nanometer size of clusters, which is critical to the low pressure

synthesis of diamond [9, 11, 67]. This might be why the hot filament reactor is as equally good as the microwave plasma reactor for the diamond synthesis even though its charge density is two or three orders of magnitude lower than that of that of the plasma reactor.

9. Microstructural criterion for cluster deposition

Experimental observation of diamond deposition with simultaneous etching of graphite [94, 95] provides a rigid proof for cluster deposition with simultaneous atomic etching; otherwise the phenomenon is against the second law of thermodynamics [10]. Also experimental observation of simultaneous deposition and etching of Si in the Si CVD process provides a rigid proof for cluster deposition with simultaneous atomic etching [18, 20]. The rigid proofs were possible because both C-H and Si-Cl-H systems have retrograde solubility of carbon and silicon, respectively, in the gas phase around the substrate temperature.

Such rigid proofs are not possible in other systems without retrograde solubility. Experimental confirmation of their existence in the gas phase can be a very strong evidence for cluster deposition. For this purpose, mass analyzers such as TOF or DMA can be used. Observation of clusters after capturing them on a TEM grid can also provide an evidence for cluster deposition. The electric bias effect on the cluster landing on a TEM grid especially in a relatively high vacuum reactor not only shows the presence of charge but also provides an evidence for cluster deposition.

An easy criterion for growth by charged clusters are the initial deposition behavior on the substrates with a high charge transfer rate (CTR) such as Pd, Pt, Rh, Ir, Ni, and

Fe. In these substrates, the porous skeletal structure develops in the initial stage of deposition because the charge is quickly transferred from the clusters to the substrate. This aspect was revealed in the diamond CVD [11, 65, 66] and in the silicon CVD (also in sputter deposition of alumina) [24].

The easiest criterion for growth by charged clusters is the evolution of ball-like or cauliflower-like microstructures, which are frequently observed in many thin film processes such as MOCVD, laser ablation and sputtering. Figures 8(a) and 8(b) show typical cauliflower-like structures of the CVD diamond and the CVD silicon, respectively. The deposition conditions for Fig. 8(a) were filament and substrate temperatures of 2000°C and 950°C, respectively, a reactor pressure of 10 Torr and a gas mixture ratio of CH_4: H_2 = 3 : 97. The deposition was done for 4 hr. The deposition conditions for Fig. 8(b) are a substrate temperature of 850°C, a reactor pressure of 100 Torr and a gas mixture ratio of SiH_4 : HCl : H_2 = 1 : 1 : 98. The deposition was done for 10 min.

In these microstructures, one big particle consists of numerous tiny nodules of tens of nanometer. It should be noted that when the methane and the silane concentrations decrease slightly to make the cluster slightly smaller, each big particle becomes a faceted single crystal as shown in Fig. 3(a). The evolution of these cauliflower-like structure cannot be explained by the atomic unit deposition. For the formation of tiny nodules shown in Figs. 8(a) and 8(b) by the atomic unit, secondary nucleation should have taken place on the growing surface. The barrier of secondary nucleation is much higher than that of growth because of the excess interface free energy between the growing surface and the nucleus. There is no growth barrier for spiral growth on screw dislocations. In the absence of screw dislocation, the growth barrier becomes a barrier

for two-dimensional nucleation.

The grain size will be determined by the growth achieved before secondary nucleation takes place. In other words, the grain size will be determined by the ratio of the secondary and the two-dimensional nucleation rates. This ratio increases with supersaturation. But the supersaturation cannot increase without limit. The kinetic roughening is the limit for the supersaturation because neither secondary nor two-dimensional nucleation can take place on the kinetically roughened surface; the rough interface undergoes ideal growth, which is controlled by diffusion without any barrier for the atomic attachment at the surface. Therefore, the ratio at the supersautration to induce kinetic roughening would determine the minimum grain size that can be achieved by the atomic growth.

Previously, Hirth and Pound [96] estimated the typical value of this ratio to be $\sim 10^{-8}$. This means that one secondary nucleation event with an incoherent boundary takes place after growth of $\sim 10^{8}$ atomic layers by two-dimensional nucleation. The estimated minimum grain size should be a few centimeters. The evolution of a cauliflower-like structure with tiny nodules of tens of nanometer cannot be explained by the atomic deposition. Therefore, the evolution of a cauliflower-like structure should be attributed to landing of nanoclusters or nanoparticles formed in the gas phase. Since a cauliflower-like structure can be observed by scanning electron microscopy (SEM), it is the easiest criterion to distinguish between atomic and cluster growth.

If this microstructural criterion is accepted as an indication of cluster growth, the possibility of crystal growth by charged clusters in the solution can be examined. It should be noted that the experimental confirmation of charged clusters in the solution is difficult because mass analyzers such as TOF or DMA cannot be used. Usually, the size

of charged clusters is below the lower limit of the analysis by light scattering. However, the crystals or films grown from the solution frequently have cauliflower-like structures or nanostructures. One example is the electrodeposited copper film for interconnects in microelectronics [97, 98].

10. Conclusion

The growth by charged clusters is a new paradigm of crystal growth. Although this paper focused on the CCM in the thin film process, it must be an important mechanism in many cases of solution growth. It should be reminded that a similar concept to the CCM had been suggested by Glasner and his collegues in the crystal growth in solution. Sunagawa's suggestion, which is similar to the CCM, is not only for gas phase growth of diamond but also for solution growth of diamond by high pressure and high temperature. Cauliflower-like structures or nanostructures, which were suggested as a microstructural evidence for cluster growth, are frequently found in the solution growth, especially in electrodeposited nanostructured films.

References

[1] P. Bennema and G. H. Gilmer, in "Kinetics of Crystal Growth" (North-Holland Publ. Co., Amsterdam 1973).

[2] J. P. van der Eerden, in "Crystal Growth Mechanism" (Vol. 1, North-Holland, Amsterdam 1993).

[3] A. Glasner and J. Kenat, J. Cryst. Growth 2 (1968) 119-127.

[4] A. Glasner and S. Skurnik, Israel J. Chem. 6 (1968) 69-72.

[5] A. Glasner and M. Tassa, Israel J. Chem. 12 (1974) 817-826.

[6] A. Glasner and M. Tassa, Israel J. Chem. 12 (1974) 799-816.

[7] G. D. Botsaris and R. C. Reid, J. Chem. Phys. 47 (1967) 3689-3690.

[8] I. Sunagawa, J. Crystal Growth 99 (1990) 1156-1161.

[9] N. M. Hwang, J. H. Hahn, and D. Y. Yoon, J. Crystal Growth 160 (1996) 87-97.

[10] N. M. Hwang and D. Y. Yoon, J. Crystal Growth 160 (1996) 98-103.

[11] N. M. Hwang, J. H. Hahn, and D. Y. Yoon, J. Crystal Growth 162 (1996) 55-68.

[12] K. Choi, S.-J. L. Kang, H. M. Jang, and N. M. Hwang, J. Cryst. Growth 172 (1997) 416-425.

[13] N. M. Hwang, J. Crystal Growth 198/199 (1999) 945-950.

[14] H. M. Jang and N. M. Hwang, J. Mater. Res. 13 (1998) 3527-3535.

[15] H. M. Jang and N. M. Hwang, J. Mater. Res. 13 (1998) 3536-3549.

[16] I. D. Jeon, C. J. Park, D. Y. Kim, and N. M. Hwang, J. Crystal Growth 213 (2000) 79-82.

[17] I. D. Jeon, C. J. Park, D. Y. Kim, and N. M. Hwang, Submitted to J. Crystal Growth.

[18] N. M. Hwang, J. Crystal Growth 205 (1999) 59-63.

[19] W. S. Cheong, N. M. Hwang and D. Y. Yoon, J. Crystal Growth 204 (1999) 52-61.

[20] N. M. Hwang, W. S. Cheong, and D. Y. Yoon, J. Crystal Growth 206 (1999) 177-186.

[21] I. D. Jeon, L. Gueroudji, and N. M. Hwang, Korean J. Ceram. 5 (1999) 131-136.

[22] K. S. Seo, MS Thesis, Metall. Eng., Chunbuk Univ., Chunju 1998, p. 40.

[23] M. C. Barnes, D. Y. Kim, H. S. Ahn, C. O. Lee, and N. M. Hwang, J. Crystal Growth 213 (2000) 83-92.

[24] W. S. Cheong, D. Y. Yoon, D. Y. Kim, and N. M. Hwang, J. Crystal Growth, (2000) in press.

[25] P. Gerhardt and K. H. Homann, Combust. Flame 81 (1990) 289-303.

[26] K. Hayasaki, Y. Takamura, N. Yamaguchi, K. Terashima, and T. Yoshida, J. Appl. Phys. 81 (1997) 1222-1226.

[27] Y. Takamura, N. Yamaguchi, K. Terashima, and T. Yoshida, J. Appl. Phys. 84 (1998) 5084-5088.

[28] K. Terashima, N. Yamaguchi, T. Hattori, Y. Takamura, and T. Yoshida, Pure & Appl. Chem. 70 (1998) 1193-1197.

[29] N. Yamaguchi, Y. Sasajima, K. Terashima, and T. Yoshida, Thin Solid Films 345 (1999) 34-37.

[30] H. S. Ahn, MS Thesis, School Mater. Sci. & Eng., Seoul National University,

Seoul 2000.

[31] M. Adachi, K. Okuyama, N. Tohge, M. Shimada, J. Sato, and M. Muroyama, Jpn. J. Appl. Phys. 31 (1992) L1439-L1442.

[32] M. Adachi, K. Okuyama, N. Tohge, M. Shimada, J. Sato, and M. Muroyama, Jpn. J. Appl. Phys. 32 (1993) L748-L751.

[33] M. Adachi, K. Okuyama, N. Tohge, M. Shimada, J. Sato, and M. Muroyama, Jpn. J. Appl. Phys. 33 (1994) L447-L450.

[34] M. Adachi, K. Okuyama, and N. Tohge, J. Mater. Sci. 30 (1995) 932-937.

[35] M. Adachi, K. Okuyama, T. Fujimoto, J. Sato, and M. Muroyama, Jpn. J. Appl. Phys. 35 (1996) 4438-4443.

[36] T. Seto, M. Shimada, and K. Okuyama, Aerosol Sci. Technol. 23 (1995) 183-200.

[37] T. Seto, S. Yokoyama, K. Okuyama, M. Hirose, T. Fujii, and H. Suzuki, IEICE Trans. Electron. E79-C (1996) 306-311.

[38] T. Seto, T. Nakamoto, K. Okuyama, M. Adachi, Y. Kuga, and K. Takeuchi, J. Aerosol Sci. 28 (1997) 193-206.

[39] T. Seto, A. Hirota, T. Fujimoto, M. Shimada, and K. Okuyama, Aerosol Sci. Technol. 27 (1997) 422-438.

[40] K. Okuyama, T. Fujimoto, and T. Hayashi, AIChE Journal 43 (1997) 2688-2697.

[41] C. T. R. Wilson, Phil. Trans. Roy. Soc. 189 (1897) 265.

[42] C. T. R. Wilson, Phil. Trans. Roy. Soc. 192 (1899) 403.

[43] C. T. R. Wilson, Phil. Trans. Roy. Soc. 193 (1899) 289.

[44] C. T. R. Wilson, Phil. Mag. 7 (1904) 681.

[45] J. L. Katz, F. C. Wen, T. McLaughlin, R. J. Reusch, and R. Partch, Science 196 (1977) 1203-1205.

[46] F. C. Wen, T. McLaughlin, and J. L. Katz, Science 200 (1978) 769-771.

[47] W. G. Eversole, U.S. Patent 3,030,188 (1962) April 17.

[48] N. C. Angus, H. A. Will, and W. S. Stanko, J. Appl. Phys. 2 (1968) 380.

[49] M. H. Magnusson, K. Deppert, J.-O. Malm, J.-O. Bovin, and L. Samuelson, J. Nanoparticle Res. 1 (1999) 243-251.

[50] I. Langmuir and K. H. Kingdon, Proc. Roy. Soc. London, Ser A 107 (1925) 61.

[51] S. Tang, Colloids and Surface A: Physicochemical and Engineering Aspects 157 (1999) 185-192.

[52] J. H. Fendler, Chem. Mater. 8 (1996) 1616-1624.

[53] G. Decher, Science 277 (1997) 1232-1237.

[54] M. P. Pileni, Langmuir 13 (1997) 3266-3276.

[55] C. P. Collier, T. Vossmeyer, and J. R. Heath, Annu. Rev. Phys. Chem. 49 (1998) 371-404.

[56] G. Cho, J.-S. Lee, D. T. Glatzhofer, B. M. Fung, W. L. Yuan, and E. A. O'Rear, Adv. Mater. 11 (1999) 497-499.

[57] K. T. Jung and Y. G. Shul, Chem. Mater. 9 (1997) 420-422.

[58] L. C. Boudreau, J. A. Kuck, and M. Tsapatsis, J. Membr. Sci. 152 (1999) 41-59.

[59] J. Feng, M. A. Winnik, R. R. Shivers, and B. Clubb, Macromolecules 28 (1995) 7671-7682.

[60] Y.-J. Park, D.-Y. Lee, M.-C. Khew, C.-H. Ho, and J.-H. Kim, Langmuir 14 (1998) 5419-5424.

[61] N. Dingenouts and M. Ballauff, Langmuir 15 (1999) 3283-3288.

[62] A. Taleb, C. Petit, and M. P. Pileni, Chem. Mater. 9 (1997) 950-959.

[63] M. P. Pileni, Ber. Bunsenges. Phys. Chem. 101 (1997) 1578-1587.

[64] A. K. Boal, F. Ilhan, and J. E. DeRouchey, Nature 404 (2000) 746-748.

[65] J. M. Huh, MS Thesis, Dept. Mater. Sci. & Eng., Korea Advanced Institute of Science and Technology, Daejon 1994.

[66] J. H. Hahn, N. M. Hwang, and D.Y. Yoon, J. Mater. Sci. Lett. 15 (1996) 1240-1242.

[67] N. M. Hwang, G. W. Bahng, and D. Y. Yoon, Diamond Relat. Mater. 1 (1992) 191-194.

[68] B. V. Spitsyn, L. L. Bouilov, and B. V. Derjaguin, J. Crystal Growth 52 (1981) 219-226.

[69] B. Spitsyn, L. L. Bouilov, and B. V. Derjaguin, Prog. Crystal Growth and Charact. 17 (1988) 79-170.

[70] B. V. Spitsyn, J. Crystal Growth 99 (1990) 1162-1167.

[71] D. M. Gruen, S. Liu, A. R. Krauss, J. Luo, and X. Pan, Appl. Phys. Lett. 64 (1994) 1502-1504.

[72] M. Yoshimoto, K. Yoshida, H. Maruta, Y. Hishitani, H. Koinuma, S. Nishio, M. Kakihana, and T. Tachibana, Nature 399 (1999) 340-342.

[73] A. V. Palnichenko, A. M. Jonas, J.-C. Charlier, A. S. Aronin, and J.-P. Issi, Nature 402 (1999) 162-165.

[74] N. M. Hwang and D. Y. Kim, J. Crystal Growth, (2000) in press.

[75] W. C. Saslaw and J. E. Gaustad, Nature 221 (1969) 160-162.

[76] R. S. Lewis, T. Ming, T. Ming, J. F. Wacker, E. Anders, and E. Steel, Nature

326 (1987) 160-162.

[77] J. A. Nuth, Nature 329 (1987) 589.

[78] D. B. Dove, J. Appl. Phys. 35 (1964) 2785-2786.

[79] H. Kumomi, T. Yonehara, Y. Nishigaki, and N. Sato, Appl. Surf. Sci. 41/42 (1989) 638-642.

[80] K. Tsubouchi, and K. Masu, J. Vac. Sci. Tech. A 10 (1992) 856-862.

[81] W.-K. Yeh, M.-C. Chen, P.-J. Wang, L.-M. Liu, and M.-S. Lin, Thin Solid Films 270 (1995) 462-466.

[82] P. G. Roberts, D. K. Milne, P. John, M. G. Jubber, and J. I. B. Wilson, J. Mater. Res. 11 (1996) 3128-3132.

[83] Y. Gao and J. H. Edgar, J. Electrochem. Soc. 144 (1997) 1875-1880.

[84] H. Kumomi and T. Yonehara, Mat. Res. Soc. Symp. Proc. 202 (1991) 83-88.

[85] H. Kumomi and T. Yonehara, Jpn. J. Appl. Phys. 36 (1997) 1383-1388.

[86] R. S. Wagner and W. C. Ellis, Appl. Phys. Lett. 4 (1964) 89.

[87] E. I. Givargizov, J. Crystal Growth 32 (1975) 20.

[88] A. M. Morales and C. M. Lieber, Science 279 (1998) 208.

[89] D. P. Yu, Z. G. Bai, Y. Ding, Q. L. Hang, H. Z. Zhang, J. J. Wang, Y. H. Zou, W. Qian, G. C. Xiong, H. T. Zhou, and S. Q. Feng, Appl. Phys. Lett. 72 (1998) 3458-3460.

[90] Y. F. Zhang, Y. H. Tang, N. Wang, C. S. Lee, I. Bello, and S. T. Lee, J. Crystal Growth 197 (1999) 136-140.

[91] G. Zhou, Z. Zhang, and D. Yu, J. Crystal Growth 197 (1999) 129-135.

[92] Y. F. Zhang, Y. H. Tang, H. Y. Peng, N. Wang, C. S. Lee, I. Bello, and S. T. Lee, Appl. Phys. Lett. 75 (1999) 1842-1844.

[93] N. M. Hwang, W. S. Cheong, D. Y. Yoon, and D. Y. Kim, J. Crystal Growth, (2000) in press.

[94] A. R. Badzian, T. Badzian, R. Roy, R. Messier, and K. E. Spear, Mater. Res. Bull. 23 (1988) 531-548.

[95] M. C. Salvadori, M. A. Brewer, J.W. Ager, K. M. Krishnan, and I. G. Brown, J. Electrochem. Soc. 139 (1992) 558-560.

[96] J. P. Hirth and G. M. Pound, in "Condensation and Evaporation" (Pergamon Press, Oxford 1963).

[97] I. V. Tomov, D. S. Stoychev, and I. B. Vitanova, J. Appl. Electrochem. 15 (1985) 887-894.

[98] C. Lingk and M. E. Gross, J. Appl. Phys. 84 (1998) 5547-5553.

Figure captions

Fig. 1. Mass distribution of negatively charged carbon clusters extracted from the hot filament reactor using a gas mixture of 1.5%CH_4-98.5%H_2, a reactor pressure of 6 Torr and a filament temperature of 2100°C. The distribution was measured by a Wien filter.

Fig. 2. Mass distribution of negatively charged carbon clusters extracted from the hot filament using gas mixtures of 1%CH_4-99%H_2, 1.5%CH_4-98.5%H_2, 3%CH_4-97%H_2 and 5%CH_4-95%H_2, a reactor pressure of 6 Torr and a filament temperature of 2100°C.

Fig. 3. SEM micrographs of diamond films deposited in situ during measurements of the energy distribution of charged clusters under a reactor pressure of 6 Torr at a filament temperature 2100°C for 1 hr with (a) 1%CH_4-99%H_2 and (b) 3%CH_4-97%H_2.

Fig. 4. SEM micrographs of silicon deposits after (a) 3 and (b) 30 min on the Ni substrate with a gas mixture ratio of SiH_4 : HCl : H_2 = 1 : 1 : 98 under a reactor pressure of 10 Torr at a substrate temperature of 850°C.

Fig. 5. SEM micrographs of (a) graphitic soot deposited on the Fe substrate and of (b) diamond deposited on the Si substrate in a hot filament reactor with a gas mixture of 1%CH_4-99%H_2 for 2 hr under 20 Torr at substrate and filament temperatures of 990°C and 2200°C, respectively.

Fig. 6. SEM micrographs of (a) Mo and (b) Si substrates after deposition for 3 min

under a reactor pressure of 10 Torr at a substrate temperature of 950°C with a gas mixture ratio of SiH_4 : HCl : H_2 = 3 : 1 : 96.

Fig. 7. SEM micrographs of (a) Si and (b) SiO_2 substrates after deposition for 6 min with the other conditions being the same as those for Fig. 6.

Fig. 8. SEM micrographs of cauliflower-like (a) diamond and (b) silicon.

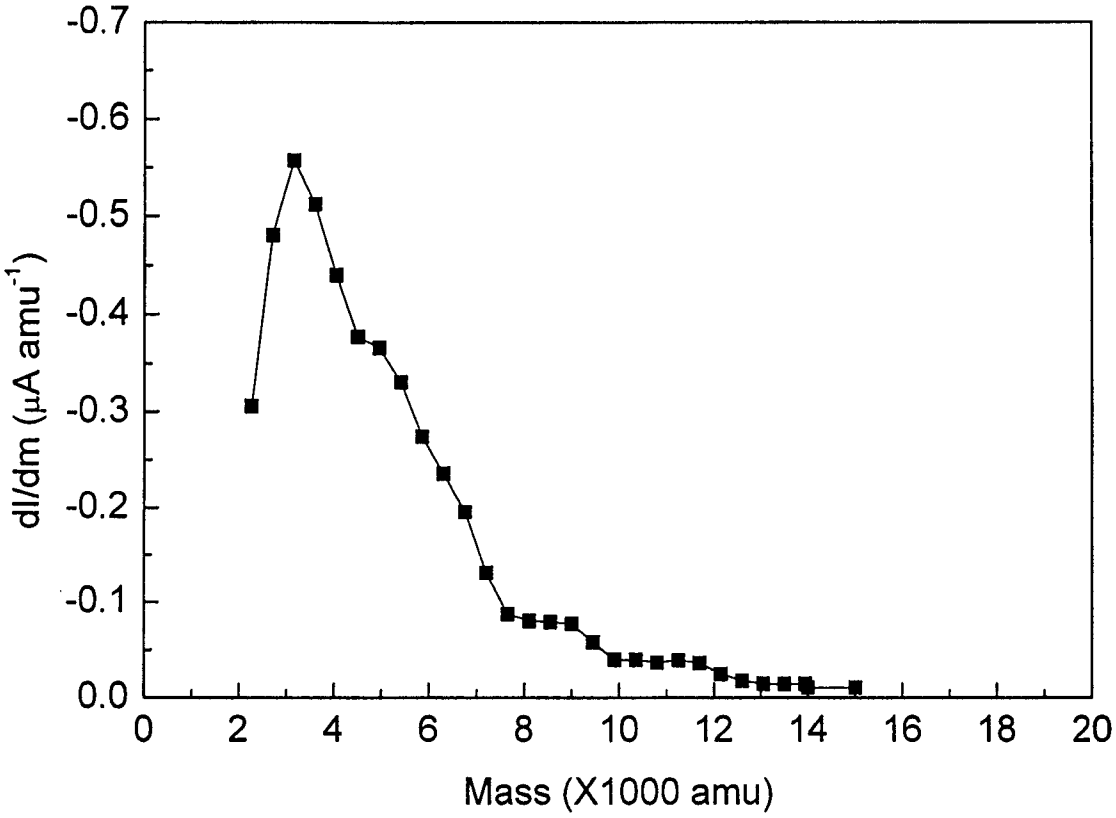

Fig. 1. Mass distribution of negatively charged carbon clusters extracted from a hot filament reactor using a gas mixture of 1.5%CH_4-98.5%H_2, a pressure of 6 Torr and a filament temperature of 2100°C. The distribution was measured by a Wien filter.

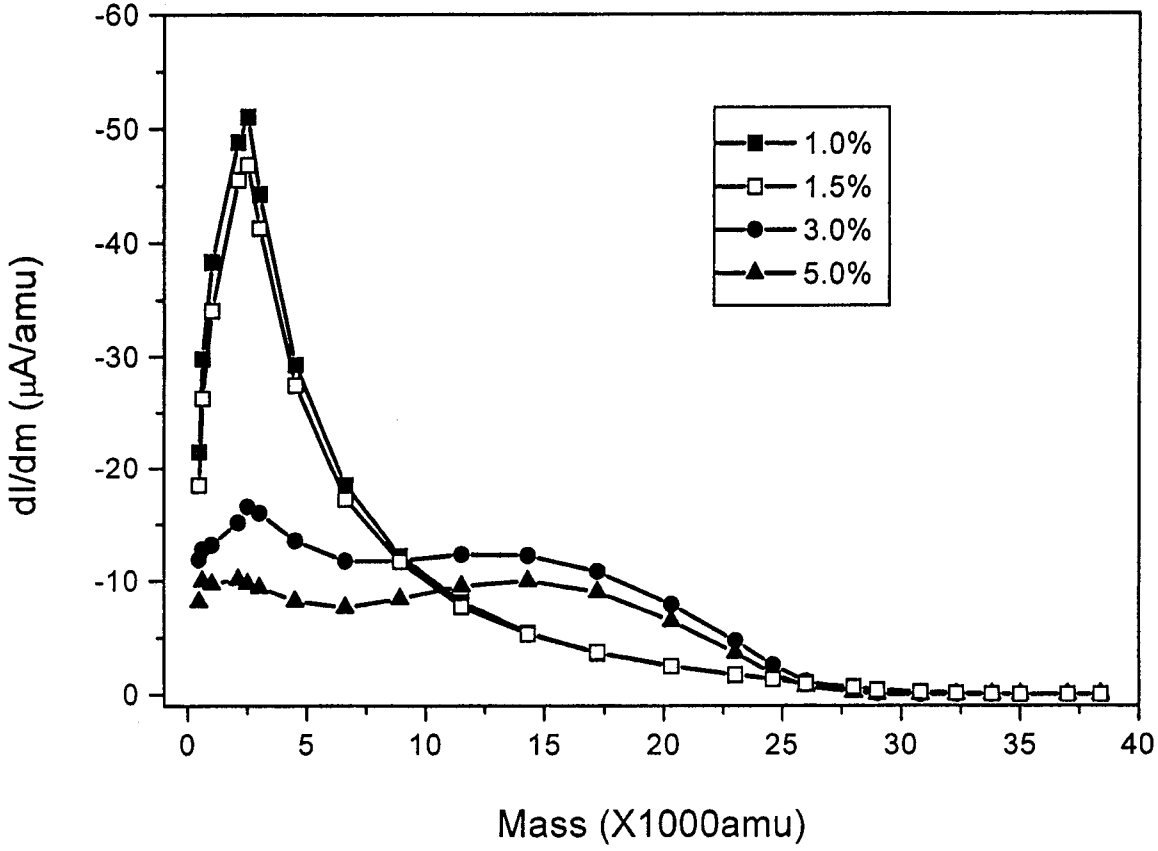

Fig. 2. Mass distribution of negatively charged carbon clusters extracted from a hot filament using gas mixtures of 1%CH_4-99%H_2, 1.5%CH_4-98.5%H_2, 3%CH_4-97%H_2 and 5%CH_4-95%H_2, a reactor pressure of 6 Torr and a filament temperature of 2100°C.

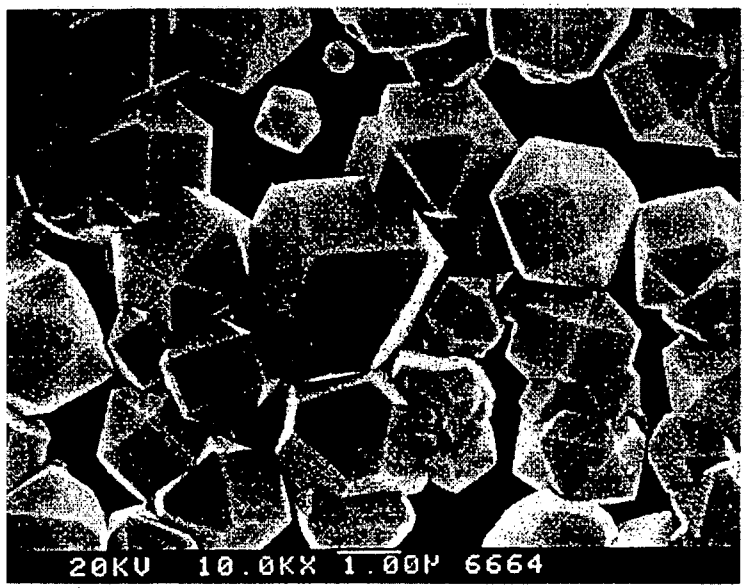

(a)

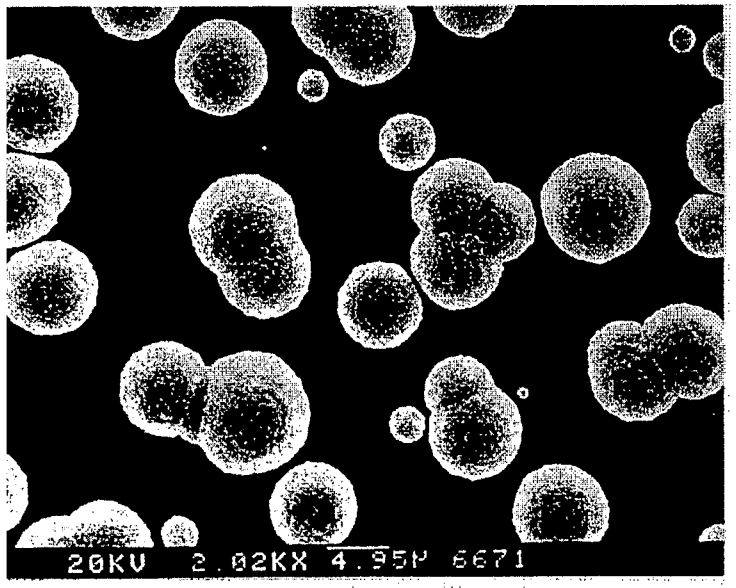

(b)

Fig. 3. SEM micrographs of diamond films deposited in situ during measurements of the energy distribution of charged clusters under a reactor pressure of 6 Torr at a filament temperature 2100°C for 1 hr with (a) 1%CH_4-99%H_2 and (b) 3%CH_4-97%H_2.

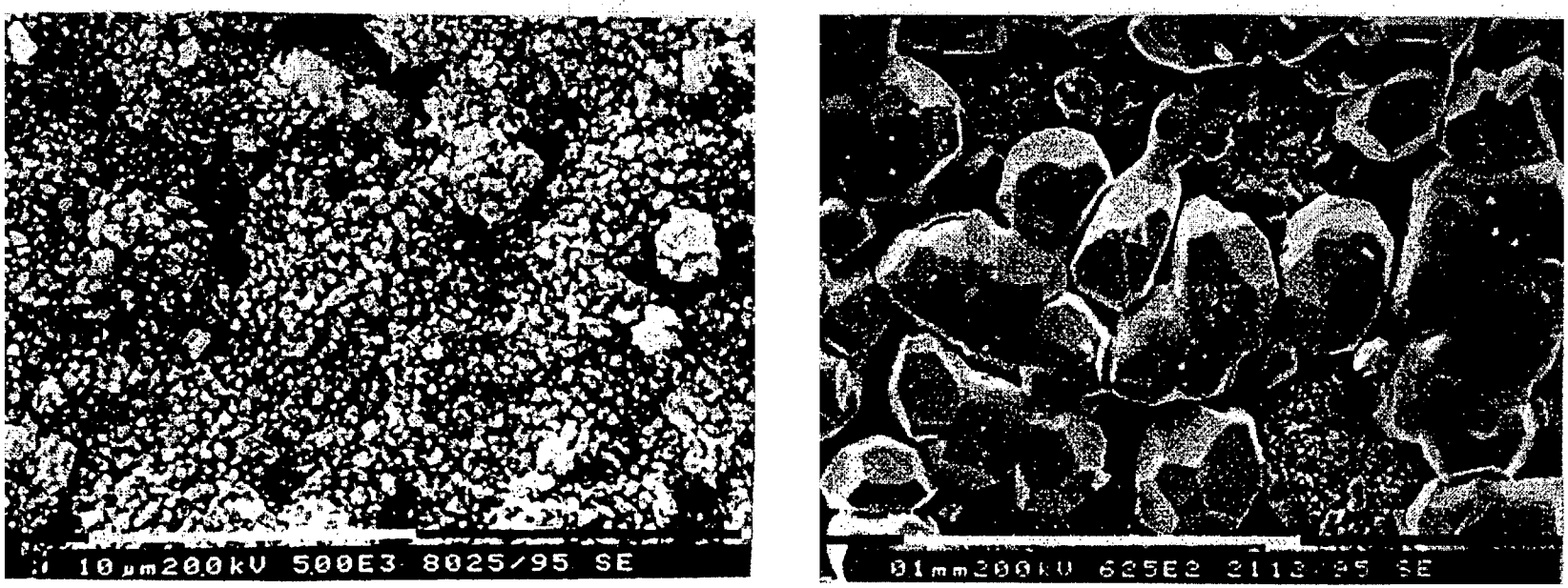

(a) (b)

Fig. 4. SEM micrographs of silicon deposits after (a) 3 and (b) 30 min on a Ni substrate with a gas mixture ratio of SiH_4 : HCl : H_2 = 1 : 1 : 98 under a reactor pressure of 10 Torr at a substrate temperature of 850°C.

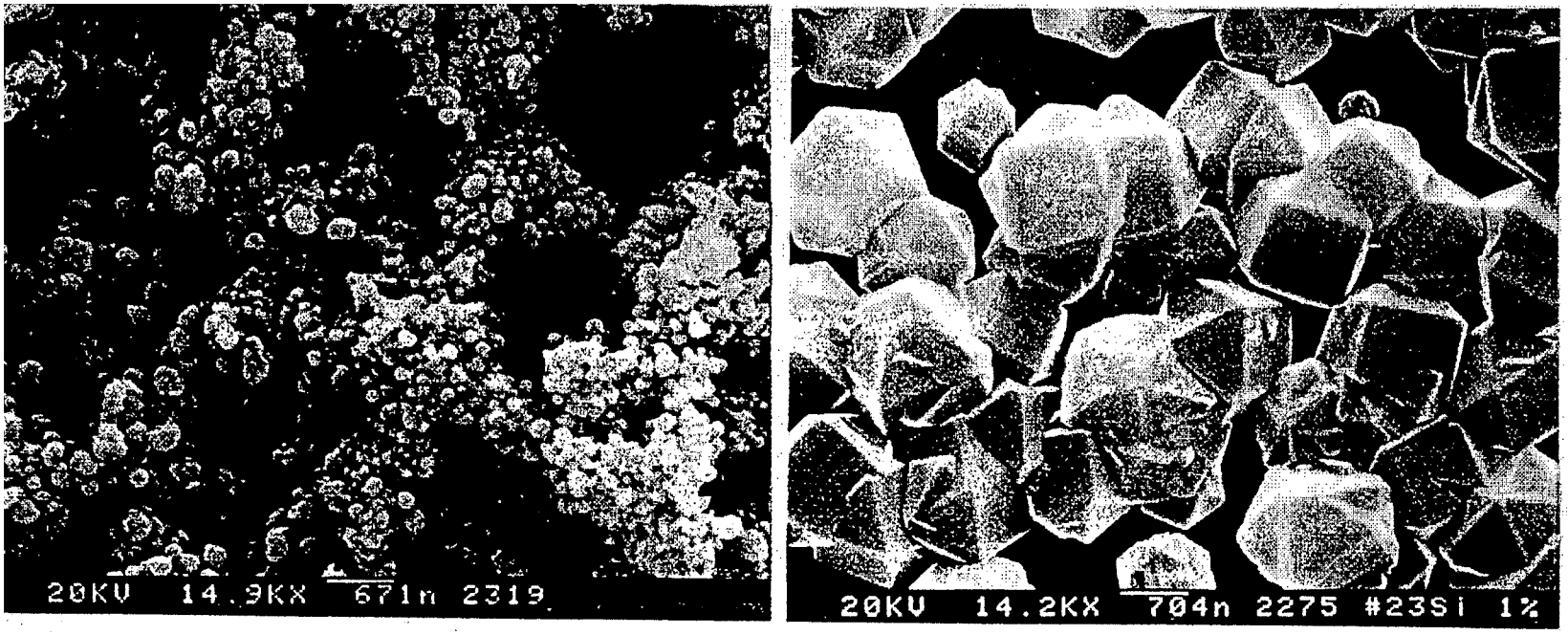

(a) (b)

Fig. 5. SEM micrographs of (a) graphitic soot deposited on a Fe substrate and of (b) diamond deposited on a Si substrate in a hot filament reactor with a gas mixture of 1%CH_4-99%H_2 for 2 hr under 20 Torr at substrate and filament temperatures of 990°C and 2200°C, respectively.

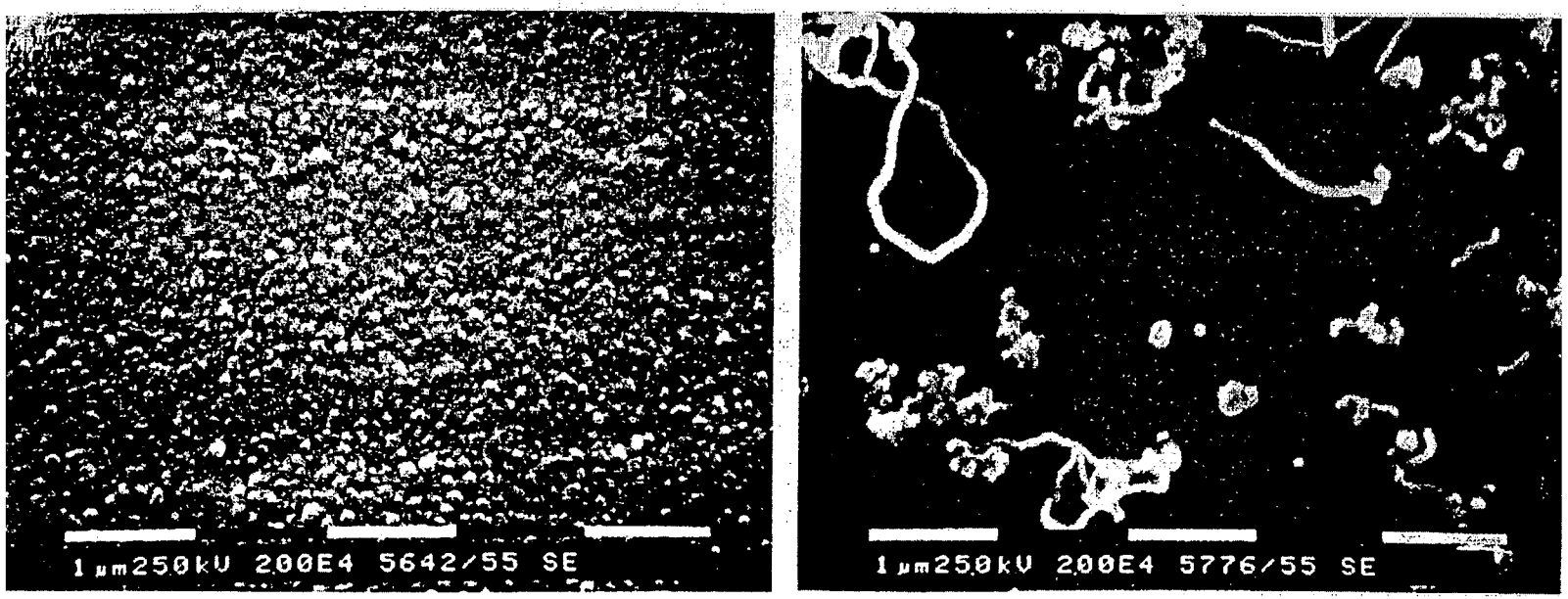

(a) (b)

Fig. 6. SEM micrographs of (a) Mo and (b) Si substrates after deposition for 3 min under a reactor pressure of 10 Torr at a substrate temperature of 950°C with a gas mixture ratio of SiH_4 : HCl : H_2 = 3 : 1 : 96.

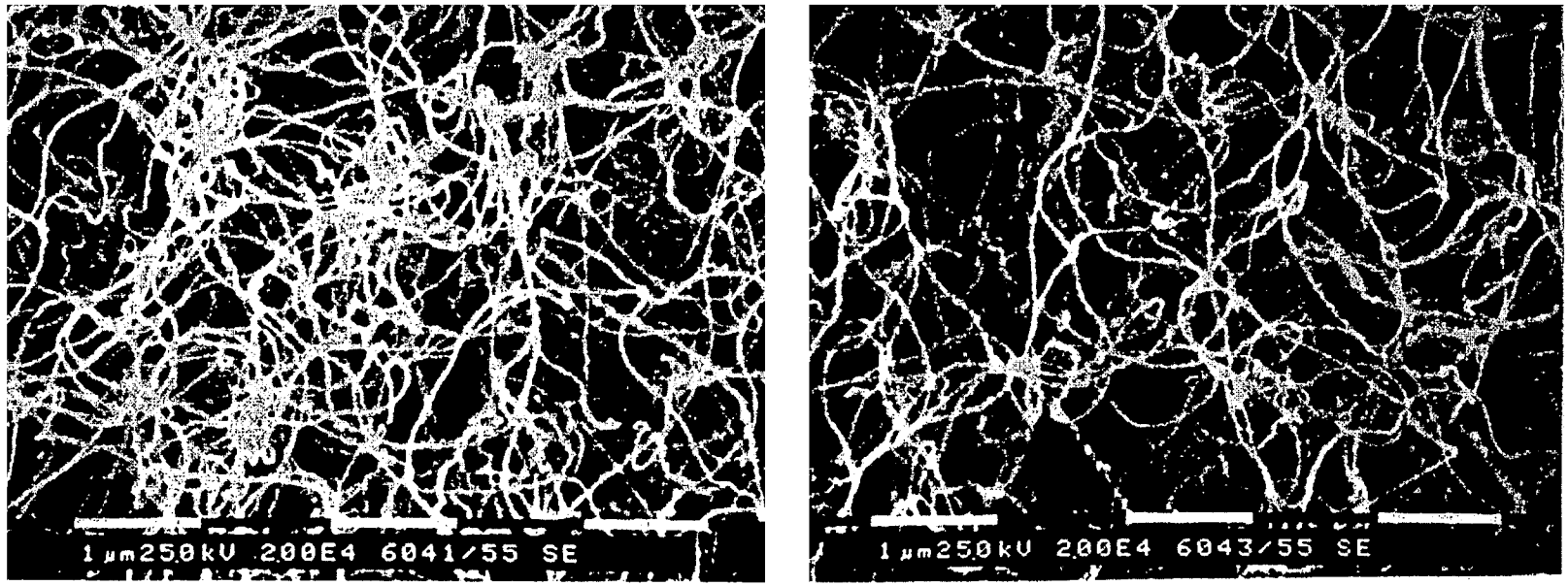

(a) (b)

Fig. 7. SEM micrographs of (a) Si and (b) SiO_2 substrates after depositioin for 6 min with the other conditions being the same as those for Fig. 6.

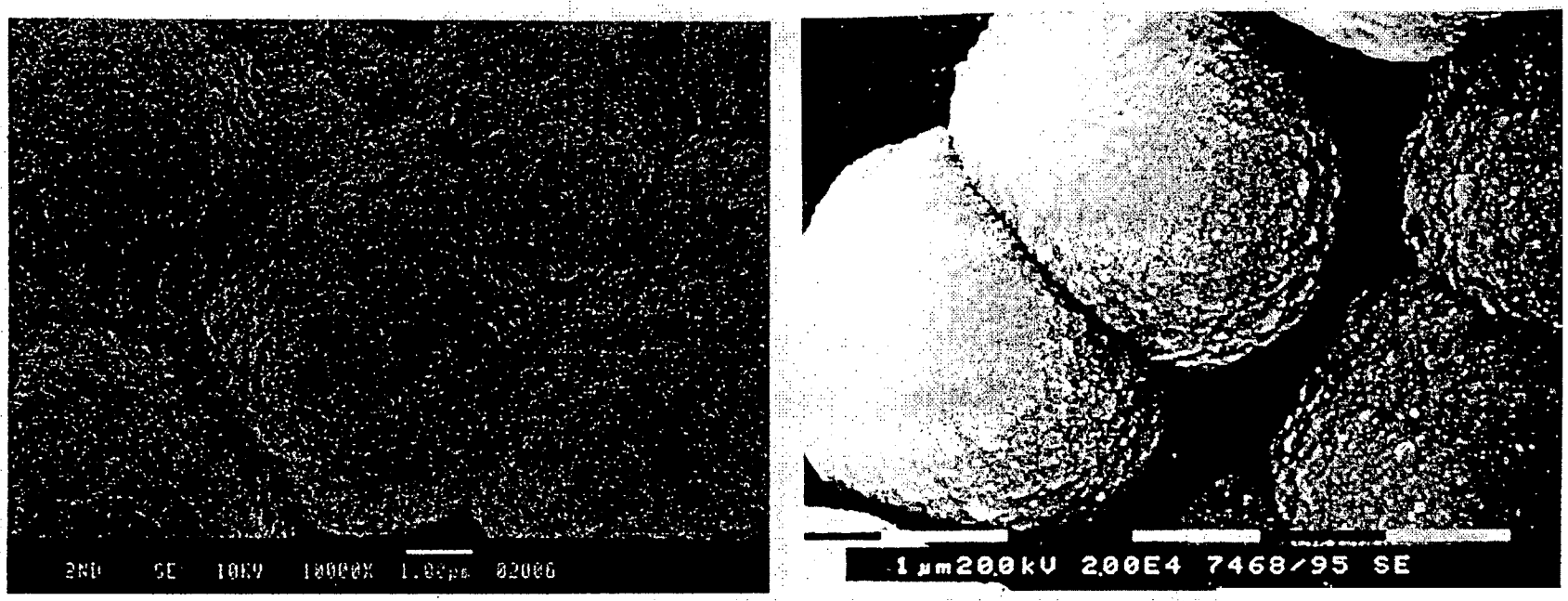

(a) (b)

Fig. 8. SEM micrographs of cauliflower-like (a) diamond and (b) silicon.